Electronic supplementary information for publication

Potent and selective inhibition of T-cell protein tyrosine phosphatase(TCPTP) by a dinuclear copper(II) complex

Caixia Yuan,[a] Miaoli Zhu,*[a,c] Qingming Wang,[a] Liping Lu,*[a] Shu Xing,[b] Xueqi Fu,*[b] Zheng Jiang,[c] Shuo Zhang [c], Zongwei Li,[d] Zhuoyu Li,[d] Ruiting Zhu,[a] Ling Ma,[a] Liqing Xu [a]

[a]Institute of Molecular Science, The Key Laboratory of Chemical Biology and Molecular Engineering of Education Ministry, Shanxi University, Taiyuan 030006, China (luliping@sxu.edu.cn, miaoli@sxu.edu.cn)

[b]Edmond H. Fischer Signal Transduction Laboratory, College of Life Sciences, Jilin University, Changchun 130023, China (fxq@jlu.edu.cn)

[c]Shanghai Synchrotron Radiation Facility, Shanghai Institute of Applied Physics, Chinese Academy of Sciences, Shanghai, P.R. China.

[d]Institute of Biotechnology, Key Laboratory of Chemical Biology and Molecular Engineering of the Education Ministry, Shanxi University, Taiyuan, Shanxi 030006, P.R. China

Figure S1 ESI-MS spectrum of ***1*** in methanol aqueous solution (1:9, v:v).

Figure S2 ORTEP view with 30% probability level of ***1*** showing atom labeling. H atoms, solvent molecules and counter-ions omitted for clarity.

Figure S3 X-band EPR spectrum for ***1*** at 25ºC.

Figure S4 Thermal analysis curves (TG and DTA) of ***1***

Figure S5 UV-Vis spectra of ***1*** recorded at 37ºC in MOPS buffer over 3 h with 10 min intervals.

Figure S6 Lineweaver-Burk plot of 1/*v* versus the reciprocal of the *p*-NPP concentration at five concentrations of inhibitor for TCPTP (I-IV). (I) $CuCl_2$; (II) $Cu(phen)Cl_2$; (III) $Cu(phen)_2Cl(ClO_4)\cdot 0.5H_2O$; (IV) Cu^{2+}-IDA system.

Figure S7 K_i determination for inhibitor against TCPTP. (I) ***1*** ; (II) $CuCl_2$; (III) $Cu(phen)Cl_2$; (IV) $Cu(phen)_2Cl(ClO_4)\cdot 0.5H_2O$; (V) Cu^{2+}-IDA system.

Figure S8 UV-vis spectrum of titrations of $Cu(NO_3)_2$ (2 ml, 10^{-4} M) with IDA (10^{-2} M) used in the study in aqueous at room temperature.

Figure S9 The fluorescence spectra of TCPTP in MOPS buffer upon addition of Na_3VO_4 (solid line) and ***1*** (dash line). Conditions: λ_{ex} = 280 nm. $E_x = E_m$ = 10 nm, 37ºC, [TCPTP] = 1.1×10^{-7} M, [Na_3VO_4]: (a) to (n), 0, 0.2, 0.4, 0.6, 0.8, 1.0, 1.2, 1.4, 1.6, 1.8, 2.0, 2.2, 2.4, 2.6(10^{-7} M), [***1***]: (o) to (z), 0.2, 0.4, 0.6, 0.8, 1.0, 1.2, 1.4, 1.6, 1.8, 2.0, 2.2, 2.4(10^{-7} M), respectively.

Figure S10 (A) Inhibitory effect of ***1*** on the viability of C6 glioma cells for 12, 24, 36 and 58h evaluated by MTT. Each value represents the mean ± SD, n=6. **p*<0.001, ***p*<0.05 (***1*** vs control at different time, respectively) (B) Comparison of cell viability between ***1*** with cisplatin, $Cu(NO_3)_2$ and ligands for 36 h. Cells were treated without (control) or with 10^{-8}, 10^{-7}, 10-^{6}, 10^{-5}M ***1***, cisplatin, $Cu(NO_3)_2$ (the concentration is double of ***1*** because of ***1*** containing two Cu atoms) and ligands (containing three times 1,10-phenanthrolin and equal iminodiacetic acid compared with ***1*** because of ***1*** containing three 1,10-phenanthrolin and one iminodiacetic acid). **p*<0.001, ***p*<0.05 (***1***, $Cu(NO_3)_2$ and ligands vs control, respectively), $^{\#}p$<0.001(***1*** vs cisplatin, $Cu(NO_3)_2$, and ligands).

Figure S11 Results of flow cytometric cellular apoptosis of C6 glioma cells untreated and treated with ***1*** (4 μM), ligands (12 μM 1,10-phenanthrolin + 4μM iminodiacetic acid) and $Cu(NO_3)_2$ (8 μM) for 36 h. The upper right quadrant B2 represented for cells in late apoptosis, the upper left quadrant B1 for necrosis cells, the lower right quadrant B4 for cells in early apoptosis and the lower left quadrant B3 for normal cells.

S1 Reactants and physical measurements

All reagents and solvents were purchased commercially and used as supplied. Double distilled water was used to prepare buffer solutions.

Elemental analyses were carried out by a VARI-EL elemental analyzer (EA). The X-ray data were collected on a Bruker SMART APEX 1K CCD diffractometer. Electron paramagnetic resonance spectrum (EPR) was obtained on a Bruker-ER 200-D-SRC spectrometer at RT. Thermal analysis curves (TG and DTA) were obtained from a TA2000/2960 thermal analyzer. Electrospray ionization mass spectrum (ESI-MS) was recorded on a Quattro Micro API (Water, USA) in methanol/aqueous solution (1:9, v:v). UV/Vis spectra were recorded on a Hewlett-Packard HP-8453 Chemstation spectrophotometer. Fluorescence emission spectra were recorded on a Cary Eclipse Spectrophotometer (Varian, USA). Bioactivity assays of the complexes were carried out on a Bio-RAD model 550 microplate reader for IC_{50} and a Hewlett-Packard HP-8453 Chemstation spectrophotometer for K_i. Apoptosis of C6 rat glioma cells were determined on FC 500 flow cytometer (Beckman-Coulter, USA).

S2 Synthesis and characterization of *[Cu$_2$(μ-IDA)(phen)$_3$(NO$_3$)]NO$_3$·4H$_2$O, 1*

S2.1 Synthesis

1,10-Phenanthroline 0.0793 g (0.4 mmol), iminodiacetic acid 0.0266 g (0.2 mmol) and $Cu(NO_3)_2{\cdot}3H_2O$ 0.0966 g (0.4 mmol) were dissolved in a water/methanol (v/v, 2:1) solution. The mixture was refluxed for 30 min with constant stirring and then cooled slowly. Filtration was kept at room temperature in two weeks. Blue crystals were obtained, filtered off and then air-dried (Yield 55%). Anal. data for $C_{40}H_{37}Cu_2N_9O_{14}$([$Cu_2$(μ-IDA)(phen)$_3$($NO_3$)]$NO_3{\cdot}4H_2O$): calcd (%): C 48.29, H 3.75, N 12.67; found (%): C 48.76, H 3.61, N 12.64; ESI-MS: m/z, 302.2(60%), 399.6(100%), 485.5(20%); calcd. [***1***-NO_3^--$4H_2O$+2Na^+]$^{3+}$ 302.3, [***1***-2NO_3^--$4H_2O$]$^{2+}$ 399.4, [***1***-2NO_3^-+$2H_2O$+2CH_3OH]$^{2+}$ 485.5.

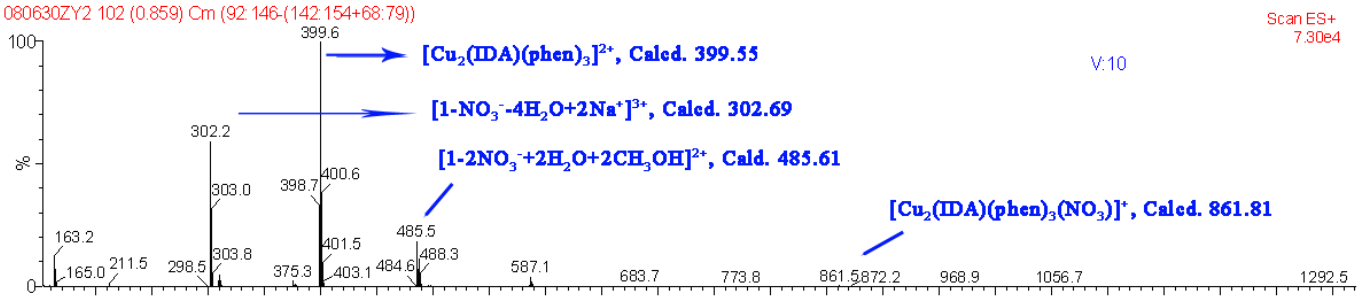

Figure S1. ESI-MS spectra of ***1*** in methanol aqueous solution (1:9, v:v).

S2.2 Crystal structure refinements

Single crystals of ***1*** is mounted on a glass fiber and used for data collection. Cell constants and an orientation matrix for data collection were obtained by least-squares refinement of diffraction data using a bruker SMART APEX CCD automatic

diffractometer. Data were collected at 25ºC using Mo *K*α radiation (λ=0.71073Å) and the *ω*-scan technique, and corrected for Lorentz and polarization effects (SADABS). The structure was solved by direct methods (SHELXS-97) and subsequent difference Fourier map and then refined on F^2 by a full-matrix least–squares procedure using anisotropic displacement parameters. ISOR instruction was employed to have ellipsoids of sites (O8 O9 O10 C29 O14 C14 O1 C18) and DFIX and FLAT were used to have nitrate (O8 N9 O9 O10) to be restraint to more appropriate values. So, 55 restraints were used for refinement anisotropically. After several cycles of refinement, all hydrogen atoms attached C and N atoms were located at their calculated positions (C_{sp2}-H, 0.93Å, C_{sp3}-H, 0.97Å, and N_{sp3}-H, 0.92Å) and were refined using a riding model. H atoms attached to O (water) were located from difference Fourier maps and refined as riding in their as-found positions with Uiso(H) = 1.5Ueq(O). Molecular graphics are from SHELXTL.[S3]

S2.3 Crystal data

1: $C_{40}H_{37}Cu_2N_9O_{14}$ (*M*r = 994.87, $[Cu_2(\mu\text{-IDA})(phen)_3(NO_3)]NO_3{\cdot}4H_2O$). Crystal dimension: 0.40 × 0.20 × 0.05 mm; monoclinic, $P2_1/c$; a = 12.509(2), b = 15.315(3) and c = 21.513(3) Å, $\alpha = \gamma = 90.0$, $\beta = 95.696(3)°$, V = 4101.0(12) Å^3, Z = 4, ρ_{calc} = 1.611 g cm^{-3}, μ = 1.119, Mo*K*α(λ = 0.71073 Å), T = 25º C; $2\theta_{max}$ = 45.6°, R_{int} = 0.065**,** R_1 = 0.094, wR_2 = 0.190 for I > 2σ(I); residual electron density: 0.642 and -0.463 eÅ^{-3}. The data collection, and the solution and refinement of the structure see S5 crystal structure refinements(ESI). CCDC 656563 contains the supplementary crystallographic data for this paper. The data can be obtained free of charge via www.ccdc.cam.ac.uk/conts/retrieving.html (or from the Cambridge Crystallographic Data Centre, 12 Union Road, Cambridge CB21EZ, UK; fax: (+44) 1223-336-033; or deposit@ccdc.cam.ac.uk) or authors.

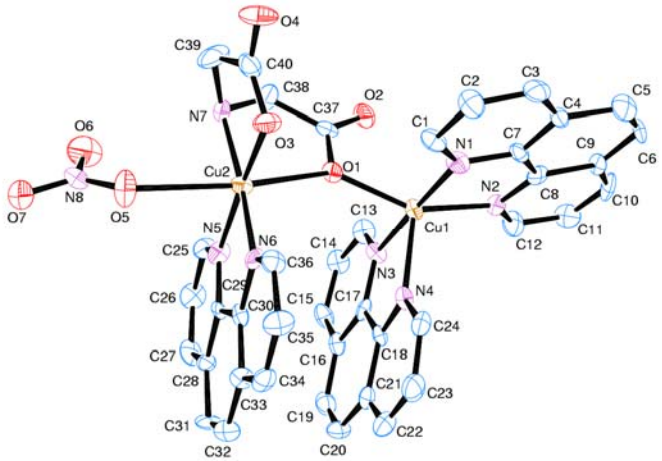

Figure. S2 ORTEP view with 30% probability level of ***1*** showing atom labeling. H atoms, solvent molecules and counter-ions omitted for clarity. The coordination polyhedron around Cu1 can be described as a distorted trigonal bipyramid but the coordination geometry around Cu2 is a distorted octahedron by a bidentate phen ligand, an O atom of nitrate ligand and an O, N, O'-tridentate chelating IDA ligand.

S2.4 EPR

The X-band EPR spectra of solid sample ***1*** at 25ºC is shown in Figure S3. The complex shows a typical axial spectrum with five well defined lines ($g_{//} > g_{\perp} > 2.0$) and the parameters ($g_{//} = 2.135$ and $g_{\perp} = 2.08$) are obtained from the simulated spectrum. These results are in agreement with the X-ray structure, which also shows the existence of a distorted trigonal bipyramidal or distorted octahedral geometries. Furthermore, the spectrum of ***1*** reveals an additional signal at "half-field" (~1600 G) which can be assigned to the S = 1 transition and is in agreement with a weak magnetic coupling as demonstrated through magnetic measurements.[S1]

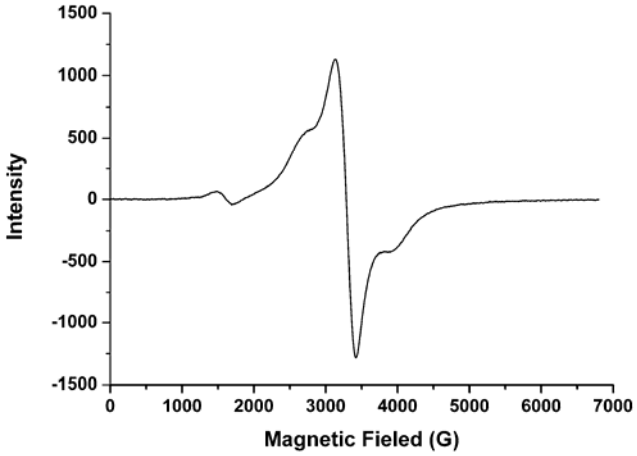

Figure S3 X-band EPR spectrum for ***1*** at 25ºC

S2.5 TG & DTA

Thermal behavior of ***1*** was studied by DTA and TG in the temperature range 30-790℃ in the static atmosphere of air (Figure S4). The complex dehydrates between 30-125℃ with a mass lose of 6.9% (calc. 7.2%) accompanied by an endothermic DTA peak at 102℃. A sharp weight loss (observed 11.2%) occurred in the temperature range 202-255℃ with an extremely exothermic DTA peak at 228 ℃, corresponding to the decomposition of IDA with remain of bridged O (calc. 11.7 %). The farther decomposition of the structure occurs between 255-790℃ with an extremely exothermic DTA peak at 352℃.

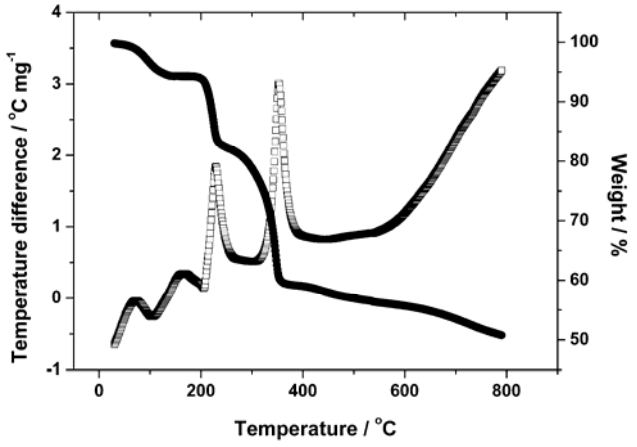

Figure S4 Thermal analysis curves (TG and DTA) of ***1***·$4H_2O$.

S2.6 UV-vis spectra of *1* in assay buffer

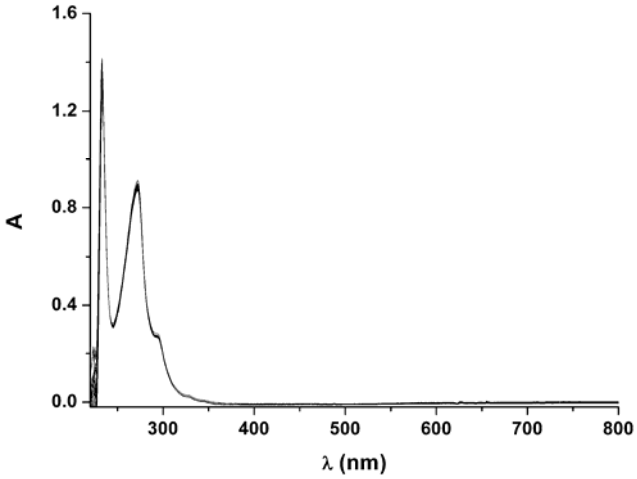

Figure S5 UV-vis spectra of ***1*** recorded at 37ºC in MOPS buffer over 3 h with 10min intervals.

S3 PTPs expression and purification

TCPTP (T-cell protein tyrosine phosphatase) and SHP-1 (Src homology phosphatase 1) enzymes were expressed and purified as reference S2a, and PTP1B (protein tyrosine phosohatase 1B) as reference S2b. SHP-2 (Src homology phosphatase 2) constructed as the pT7-ΔSHP2 expression vetcor containing human SHP-2 catalytic domain was expressed and purified as almost the same procedure as that for SHP-1. HePTP (hematopoietic protein tyrosine phosphatase), constructed as the pGEX-4T-GST-ΔHePTP expression vetcor containing human HePTP catalytic domain was also expressed and purified as the same as above PTPs. The only difference was that the supernatant was directly loaded to an Glutathione-Sepharose 4B column and eluted with washing buffer 1 (25mM Tris, 2mM 2-ME, 0.15mM NaCl, 2mM EDTA, 0.1% Triton X-100, pH 8.0), washing buffer 2 (25mM Tris, 2mM 2-ME, 0.15mM NaCl, 2mM EDTA, pH 8.0) and Elution buffer (50mM Tris, 10mM Glutathione, pH 8.0), respectively.

S4 PTP inhibition assays

The assays were performed in 20mM 3-morpholinorpro-phanesulfonic acid (MOPS) buffer, pH7.2, containing 50mM NaCl. The complexes were dissolved in dimethyl sulfoxide (DMSO) (10^{-2}M), and diluted to various concentrations, then further diluted 10 times into enzyme-MOPS buffer solutions for activity studies. Inhibition assays were performed in the same buffer on a 96-well plate in 100μL volumes. The enzyme and complex were preincubated for 30 min prior to the initiation of the enzymatic reaction by the addition of the substrate *p*-nitrophenol phosphate (*p*NPP). Then the assays were terminated by the addition of 5μL of 2M NaOH. A_{405} was measured on a microplate reader. Solution of the copper complex was freshly prepared before each experiment. Kinetic parameters, including the inhibition constant (K_i), Michaelis constant (K_m) and maximal velocity (V_m), were determined *via* the Lineweaver-Burk plot method at increasing concentration of substrate (0.2, 0.3, 0.5, 1.0, 2.0, 4.0 and 8.0 mM) and the inhibitor (0, 20, 50, 80, 100 nM).

The control experiments for the kinetic analysis of Cu^{2+}, complexes of Cu^{2+}:Phen (1:1 and 1:2, respectively) and the complex of Cu^{2+}- IDA (1:1) system inhibiting TCPTP (Figure S6 and S7), were carried out to compare with the inhibition model of ***1***. The complexes $Cu(phen)Cl_2$ and $Cu(phen)_2Cl(ClO_4)\cdot 0.5H_2O$ was prepared as previously described. [S4-S5] Anal. data for $C_{12}H_8Cl_2CuN_2$: calcd (%): C 45.80, H 2.56, N 8.90; found (%): C 45.58, H 2.31, N 8.91, and anal. data for $C_{24}H_{17}Cl_2CuN_4O_{4.5}$: calcd (%): C 50.76, H 3.02, N 9.87; found (%): C 50.63, H 3.24, N 9.79. The Cu^{2+}-IDA system was prepared by mixing $Cu(NO_3)_2$ with IDA in aqueous solution. The solution was directly used for TCPTP inhibition assays. In order to confirm the formation of the Cu^{2+}-IDA complex, UV-vis titration was performed. As shown in Figure S8, Cu^{2+}-IDA (1:1) complex was formed.

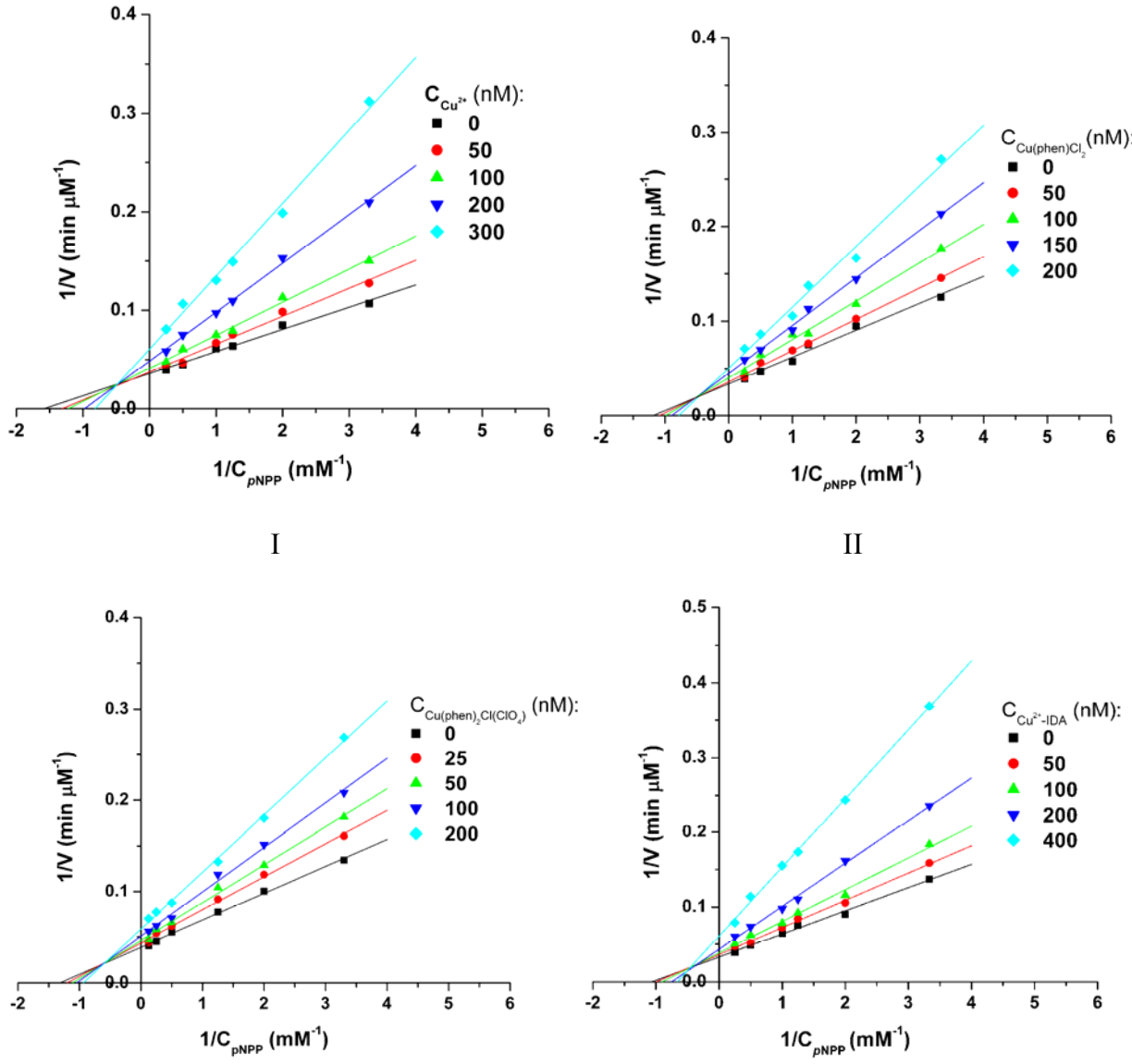

I II

III IV

Figure S6. Lineweaver-Burk plot of 1/*v* versus the reciprocal of the *p*-NPP concentration at five concentrations of inhibitor for TCPTP (I-IV). (I) $CuCl_2$; (II) $Cu(phen)Cl_2$;(III) $Cu(phen)_2Cl(ClO_4)\bullet 0.5H_2O$; (IV) Cu^{2+}-IDA system.

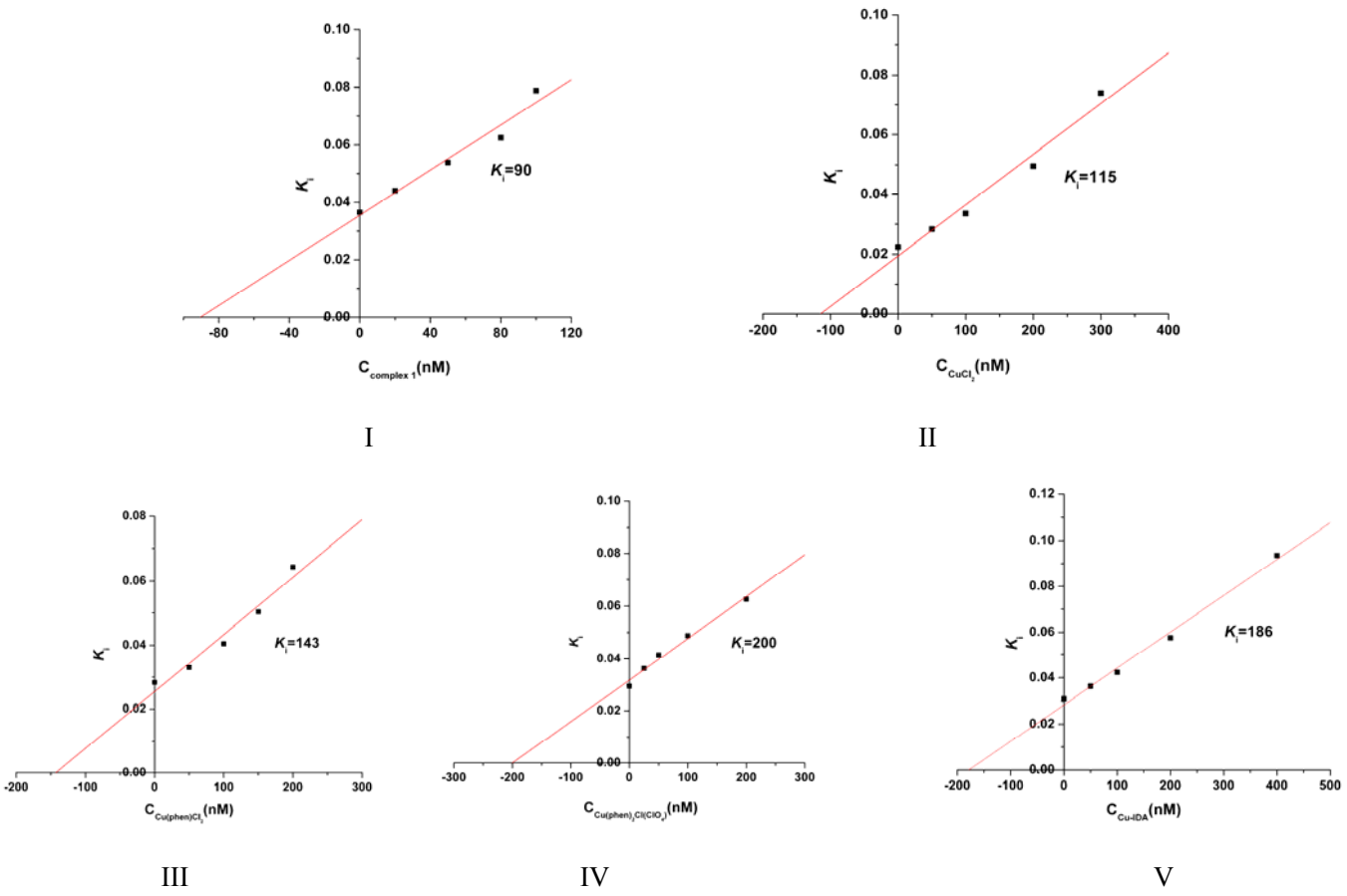

Figure S7. K_i determination for inhibitors against TCPTP. (I) ***1*** ; (II) $CuCl_2$; (III) $CuphenCl_2$;(IV) $Cu(phen)_2Cl(ClO_4)\cdot 0.5H_2O$; (V) Cu^{2+}-IDA system.

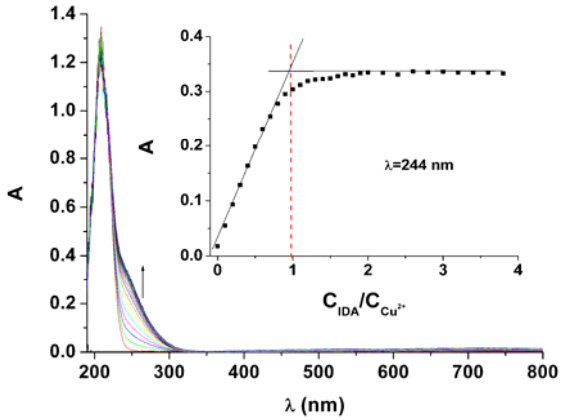

Figure S8 UV-vis spectra of titrations of $Cu(NO_3)_2$ (2ml, 10^{-4}M) with IDA (10^{-2} M) used in the study in aqueous at room temperature.

S5 The binding constant and the stoichiometry calculations.

Maximum fluorescence intensities of TCPTP without and with the quencher (F_0 and F, respectively) were determined and F_0/F values were plotted against the quencher complex ***1***. The experimental data were fitted with the Stern–Volmer equation (1): [S6]

$$\frac{F_0}{F} = 1 + k_q \tau_0 [Q] = 1 + k_{sv}[Q] \qquad (1)$$

where F_0 and F are the fluorescence intensities before and after the addition of the quencher, respectively. K_{SV} is the Stern–Volmer quenching constant and [Q] is the concentration of quencher. k_q is the quenching rate constant of the TCPTP and $k_q = K_{SV}/\tau_0$. τ_0 is the average lifetime of the protein without any quencher. The fluorescence lifetime for proteins is ~ 10^{-8} s.[S7] The binding constants and the stoichiometry between TCPTP and quencher (complex ***1***) were calculated from the static quenching equation (2) by plotting lg ((F_0-F)/F) vs lg [Q]:[S8]

$$\lg\frac{F_0 - F}{F} = \lg K + n\lg[Q] \qquad (2)$$

Where K is the binding constant and n is the number of binding sites (stoichiometry).

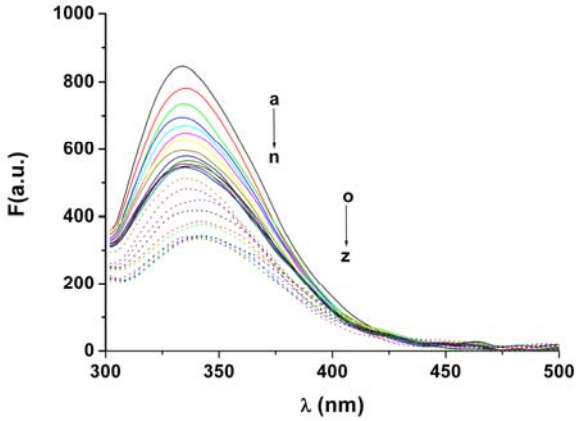

Figure S9 The fluorescence spectra of TCPTP in MOPS buffer upon addition of Na_3VO_4 (solid line) and ***1*** (dash line). Conditions: λ_{ex} = 280 nm. $E_x = E_m$ = 10 nm, T=37°C, [TCPTP] = 1.1×10^{-7} M, [Na_3VO_4]: (a) to (n), 0, 0.2, 0.4, 0.6, 0.8, 1.0, 1.2, 1.4, 1.6, 1.8, 2.0, 2.2, 2.4, 2.6(10^{-7} M), [***1***]: (o) to (z), 0.2, 0.4, 0.6, 0.8, 1.0, 1.2, 1.4, 1.6, 1.8, 2.0, 2.2, 2.4(10^{-7} M), respectively.

S6 Extended X-ray absorption fine structure (EXAFS)

S6.1 X-ray absorption spectroscopy (XAS)

The Cu K-edge X-ray absorption spectra of ***1*** solution (25 μM), {***1***(75 μM)+TCPTP(93 μM)} mixing solution and {$CuCl_2$(75 μM)+TCPTP(93 μM)} mixing solution were recorded at the SSRF (Shanghai China), beam-line 14W1. The storage ring was working at the electron beam energy of 3.5 GeV with a maximum stored current of about 210 mA. Data were recorded using a Si(111) double crystal monochromator. In the energy range selected for the experiments a detuning of the silicon crystals of 10% at the Cu K-edge was performed to suppress the high harmonics content. The energy was defined assigning the first inflection point of Cu foil spectrum to 8979 eV. The data were measured in fluorescence mode using four-element silicon drift detector.

S6.2 XAS method and EXAFS data analysis.

X-ray Absorption Spectroscopy (XAS) is a powerful technique capable to determine the local structure around a photoabsorber. It has the ability to define structural differences at a resolution commensurate with the different redox and coordination chemistry of the metal ion regardless of the physical state of sample under studied, i.e., solution, crystal and powder etc. The X-ray absorption near-edge structure (XANES) refers to the features located in the energy region around absorption edge, which is dominated by the multiple-scattering (MS) effect of the photoelectrons with coordinated atoms, thus servers as a fingerprint for identify the change of three dimensional structure around a photoabsorber.[S9]

The EXAFS data analysis has been performed using IFEFFIT[S10] package and the analyses were carried out by a standard procedure. The measured absorption spectra below the 8960 eV region were fitted to a straight line, and then the background contributions above the post-edge region, $\mu_0(E)$, were fitted to a polynomial. The background-subtracted absorption spectra were normalized for the above energy region, $\chi(E)=(\mu(E)- \mu_0(E))/ \mu_0(E)$, which is the so-called EXAFS signal. The k^2-weighted EXAFS spectra, $k^2\chi(E)$ were Fourier transformation with the k range from 1.8 to 10 $Å^{-1}$ to show the contribution of each bond pair on the Fourier transform peak.

S7 Cell biological assay

Cell culture

C6 rat glioma cell (which was a gift from Dr. Yuejun Fu, Institute of Biotechnology, Shanxi University, Taiyuan, P.R. China) was cultured in Dulbecco's modified Eagle's medium (DEME) medium supplemented with penicillin/streptomycin (100 units/ml) and 10% fetal bovine serum (FBS) and grown at 37ºC in a humidified atmosphere in the presence of 5% CO_2.

Western blotting analysis

C6 glioma cells were cultured in DMEM until mid-log phase and then incubated with 0.01, 0.1, or 1.0 μM ***1***，ligands (3.0 μM 1,10-phenanthrolin + 1.0 μM iminodiacetic acid) and 2.0 μM $Cu(NO_3)_2$ for 5 h. All samples and control contain 0.1% DMSO. After exposure, cells were harvested, washed with ice-cold 0.85% NaCl twice, and suspended in 80 μl ice-cold RIPA lysis buffer (Beyotime Institute of Biotechnology). After being incubated on ice for 20min, the cell lysates were centrifuged at 13000 rpm at 4 ºC for 15min and supernantants were collected and protein concentration was measured using a BCA Protein Assay Kit (Beyotime Institute of Biotechnology). Equal amounts of protein (80 μg) were separated by 10% SDS-polyacrylamide gels (SDS-PAGE) and transferred onto PVDF membranes (Millipore, USA). The membranes were blocked with 5% w/v non-fat dry milk for 30 min at room temperature, and incubated with primary antibody (1:500) at 4ºC overnight. Antibodies against phosphorylated Src (Y418), phosphorylated Src (Y529), Src (L412) and IgG (H+L) were purchased from Ametica Basic Gene Associate Bioscience Inc., and monoclonal rabbitanti-glyceraldehyde-3-phosphate dehydrogenase (GAPDH) was purchased from Bioworld Technology Inc.. After washing and incubation with secondary antibodies at room temperature for 2 h, protein signals were developed and visualized using a chemiluminescence system.

Cell proliferation assay

C6 glioma cells were plated in each well of 96-well plats containing DMEM with 10% FBS and cultured at 37ºC overnight. The cells were treated with various concentrations of ***1***, $Cu(NO_3)_2$, ligands or cisplatin, ranging from 10^{-8}~10^{-5} M for 12, 24, 36 and 58h. DMSO concentration was adjusted to 0.1% in all the samples and control (without the complex or cisplatin) was also included. After exposure, the cells in each well were added with 20 μl the 3-[4,5-Dimethylthiazo-2-yl]-2,5-diphenpyltetra-zolium bromide (MTT, 5mg/ml) and incubated at 37ºC for 4 h, then the medium and MTT were removed and 150 μl DMSO was added to each well. The optical density (OD) was obtained at 490 nm with microplate reader. Each data point was collected by averaging that of six wells. The cell viability rate was calculated by the following equation:

$$\text{Cell viability (\%)} = T/C \times 100 \qquad (3)$$

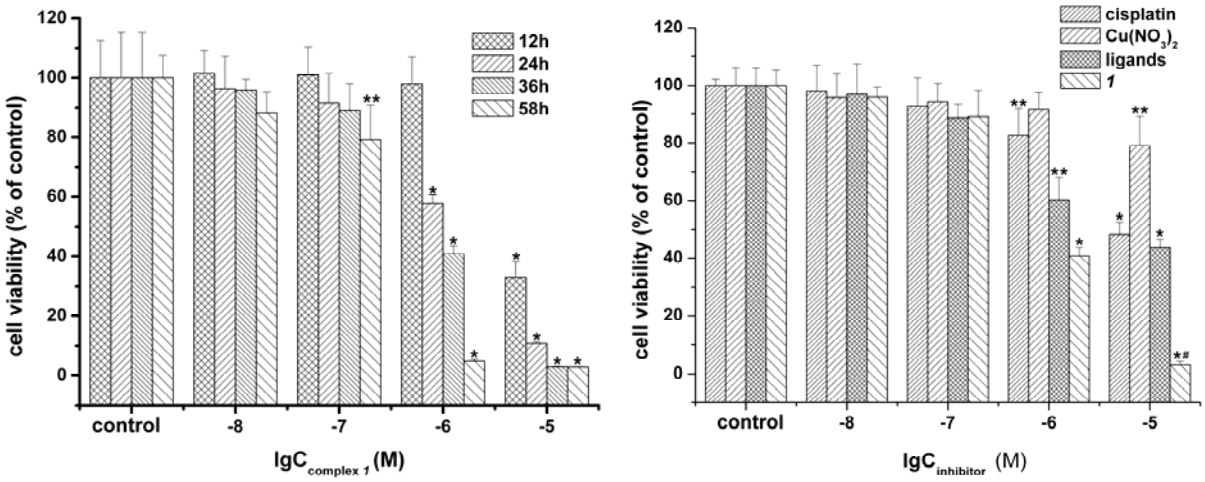

A B

Figure S10. (A) Inhibitory effect of ***1*** on the viability of C6 glioma cells for 12, 24, 36 and 58h evaluated by MTT. Each value represents the mean ± SD, n=6. **p*<0.001, ***p*<0.05 (***1*** vs control at different time) (B) Comparison of cell viability between ***1*** with cisplatin, $Cu(NO_3)_2$ and ligands for 36 h. Cells were treated without (control) or with 10^{-8}, 10^{-7}, 10-^{6}, 10^{-5}M ***1***, cisplatin, $Cu(NO_3)_2$ (the concentration is double of ***1*** because of ***1*** containing two Cu atoms) and ligands (containing three times 1,10-phenanthrolin and equal iminodiacetic acid compared with ***1*** because of ***1*** containing three 1,10-phenanthrolin and one iminodiacetic acid). **p*<0.001, ***p*<0.05 (***1***, $Cu(NO_3)_2$ and ligands vs control, respectively), $^{\#}p$<0.001(1 vs cisplatin, $Cu(NO_3)_2$, and ligands)

Cell apoptosis assessment

C6 glioma cells were treated with 4.0 μM ***1*** for 36 h. Then they were harvested and washed twice with ice-cold 0.85% NaCl and resuspended in 500 μl of 1 × binding buffer containing 5 μl of Annexin V-FITC and 5 μl of PI (KeyGEN Biotech.). After 15min incubation in the dark at room temperature, cells were analyzed for annexin V binding within 1 h with a flow cytometer. The number of viable, early apoptotic, late apoptotic and necrotic cells were quantitated by annexin V bindng and PI uptake.

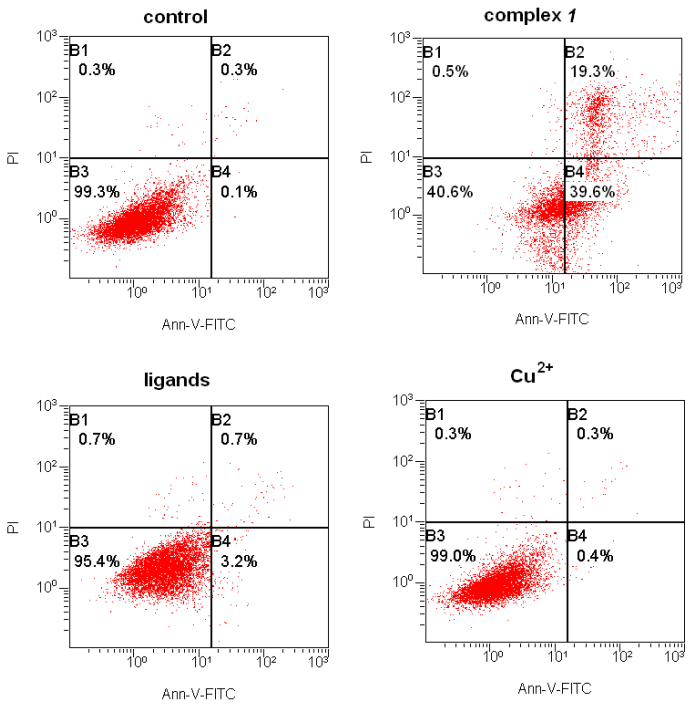

Figure S11 Results of flow cytometric cellular apoptosis of C6 glioma cells untreated and treated with ***1*** (4.0 μM), ligands (12.0 μM 1,10-phenanthrolin + 4.0 μM iminodiacetic acid) and $Cu(NO_3)_2$ (8.0 μM) for 36 h. The upper right quadrant B2 represented for cells in late apoptosis, the upper left quadrant B1 for necrosis cells, the lower right quadrant B4 for cells in early apoptosis and the lower left quadrant B3 for normal cells.

Reference

S1 R. A. Peralta, A. Neves, A. J. Bortoluzzi, A. dos Anjos, R. F. Xavier, B. Szpoganicz, H. Terenzi, M. C. B. de Oliveira, E. Castellano, G. R. Friedermann, A. S. Mangrich and M. A. Novak, *J. Inorg. Biochem.* 2006, **100**, 992.

S2 a) C. X. Yuan, L. P. Lu, X. L. Gao, Y. B. Wu, M. L. Guo, Y. Li, X. Q. Fu and M. L. Z hu, *J. Biol. Inorg. Chem.* 2009, **14**, 841; b) X. L. Gao, L. P. Lu, M. L. Zhu, C. X. Yuan, J. F. Ma and X. Q. F u, *Acta Chim. Sin.* 2009**, 67**, 929.

S3 a) G. M. Sheldrick, Correction Software, University of Gotingen (Germany) 1996; b) G. M. Sheldrick, Program for the Solution of Crystal Structure, University of Gotingen (Germany) 1997; c) G. M. Sheldrick, Program for the Refinement of Crystal Structure, University of Gotingen (Germany) 1997; d) G. M. Sheldrick, SHELXTL/PC. Version 5.1. Bruker AXS Inc., Madison, Wisconsin (USA) 1999.

S4 G. Bahr and G. Schleitzer, *Chem Ber*, 1955, **88**, 1771.

S5 Y. B. Wei and P. Yang, *Acta Cryst. E***60**, 2004, m429.

S6 O. Stern and M. Volmer, *Phys. Z.* 1919, **20,** 183.

S7 J. R. Lakowicz, G. Weber, *Biochemistry* 1973, **12**, 4161.

S8 M. Alain, B. Michel and D. Michel, *J. Chem. Edu*. 1986, **63**, 365.

S9 J. J. Rehr and A. L.Ankudinov, *Coord. Chem. Rev*. 2005, **249**,131.

S10 M. Newville, *J. Synchrotron Radiat.* 2001, **8**, 322.